(PL) spectra. The electron-hole confinement energy, PL peak intensity and width as a function of the magnetic field were studied under magnetic fields from 0 to 30 T.

Figure 1 shows the position of the peak PL and the bandwidth from porous silicon sample as a function of the magnetic field. The sample was cooled to 20 K and excited by an Argon ion laser at the wavelength of 457.9 nm. The position of the peak PL and the bandwidth represent the energy and its distribution of the band gap, respectively, during the electron-hole recombination. A blue shift in energy band gap and the reduction in bandwidth were observed when the magnetic field was increased. These results confirmed our predication that the high magnetic field can confine electron-hole orbit to have a uniform confinement energy. Besides the position of the peak PL and the bandwidth, the PL intensity under high magnetic fields was also investigated.

The observation of this study has improved the knowledge of the origin of electron-hole recombination and optical nonlinearity in quantum confinement systems. The project has also involved collaboration within the Department of Electrical Engineering and the NHMFL. The project will help to establish a long-term collaboration relationship in future researches in the field related to optical properties of materials under high magnetic fields.

KONDO / HEAVY FERMION SYSTEMS

Magnetoresistance of Low Carrier Density Hexaborides

Aronson, M.C., Univ. of Michigan, Physics

The recent discovery of ferromagnetism in La doped BaB_6 and CaB_6 (Young 1999) has renewed interest in the properties of the low density, three dimensional electron gas. While it has not yet been directly demonstrated, it is thought that stoichiometric RB_6 (R=Ca, Sr, Ba) are semimetals, with overlap of the conduction and valence bands at the X-point. It is possible to vary the band overlap, and thus the carrier concentration, by decreasing the alkali earth concentration in the starting material, or by doping with a trivalent element such as La. In the experiment reported here, we have studied five different samples of RB_6 that are expected to have carrier concentrations that range from that of stoichiometric RB_6 to the range of carrier concentrations for which ferromagnetism is observed in La-doped RB_6. We have carried out magnetoresistance and Hall measurements in these samples in the 60 T short pulse magnet.

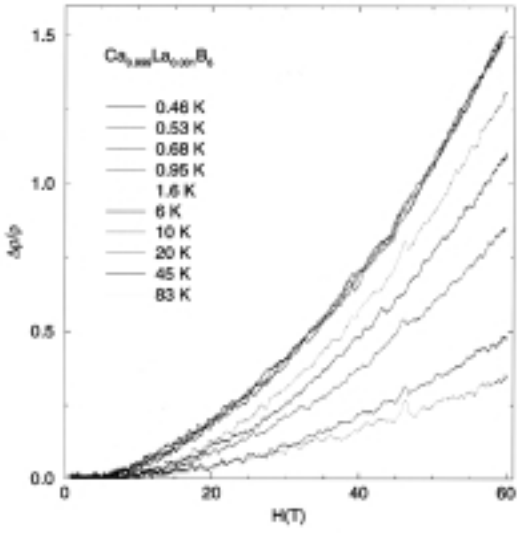

Figure 1. Magnetoresistance of CaB_6 with 0.1% La, for temperatures from 0.45 K (top) to 83 K (bottom).

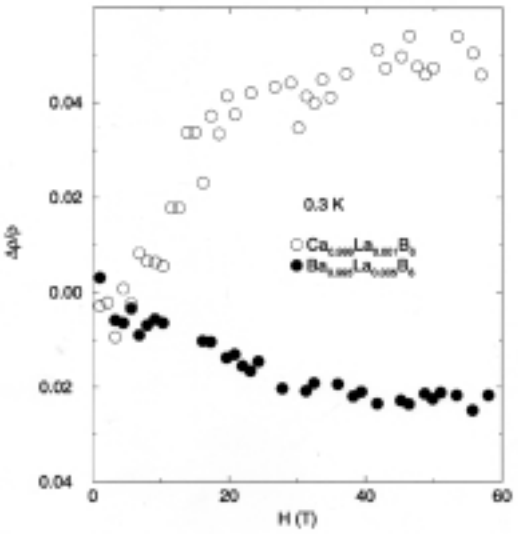

Figure 2. Comparison of the transverse magnetoresistance for two samples with different carrier concentrations.

An example of our results is given in Figure 1. We find a large positive magnetoresistance in each sample, which is approximately quadratic in field. Similar field dependences have been found in other hexaboride compounds (Cooley 1997, Aronson 1999). As in those cases, the magnitude of the magnetoresistance increases with decreasing carrier concentration, as expected from Kohler's rule. In addition to this positive magnetoresistance, we have also identified an additional contribution to the magnetoresistance in low fields, which is even more strongly sensitive to the carrier concentration of the sample. These contributions are plotted in Figure 2 for each sample. Since the magnitude of this contribution varies dramatically from sample to sample, as does the sign, we speculate that this is actually a Hall resistance. Unfortunately, we were not able to reverse the field direction to test this hypothesis.

Arko, A.J., *et al*., Phys. Rev. B, **13**, 5240 (1976).
Aronson, M.C., *et al*., Phys. Rev. B, **59**, 4720 (1999).
Cooley, J.C., *et al*., Phys. Rev. B, **52**, 7322 (1995).
Young, D.P., Nature, **397**, 412 (1999).

Proof Tests of Planar Micro-Magnetometer

Clark, R., Univ. of New South Wales, Sydney, Australia
Starrett, R., UNSW
Reilly, D., UNSW
Mielke, C.H., NHMFL/LANL
Rickel, D.G., NHMFL/LANL

We have used de Haas van Alphen measurements on two heavy fermion compounds to test the sensitivity of micro-magnetometers that have been fabricated at the UNSW nano-fabrication facility. The magnetometers are compensated inductive devices of millimeter scale size. The tests are used to determine whether there are performance benefits relative to the traditionally wound compensated solenoidal coils. The planar coils are lithograpically defined with precise placement of coil wires that should result in almost perfect compensation, i.e. much better than traditional coils. This should translate into

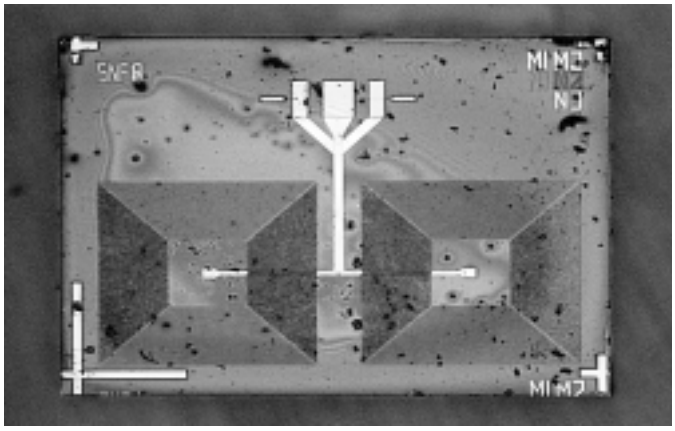

Figure 1. The lithographically deposited magnetometer. The coil size is 400 x 400 μm.

higher sensitivity magnetometers, all other things being equal. The second benefit to be derived from this coil technique is a high sample filling factor relative to the coil volume, again leading to a better signal to noise ratio. To realize these benefits, however, a much better preamplifier and shielding system must be used because these small devices inherently produce much smaller signal amplitudes. Figure 1 shows the geometry of the coil used for the present experiments. These are side by side coils, counter wound to cancel out the background field. The coil axis is perpendicular to the applied magnetic field resulting in the electron orbit planes also being perpendicular to the magnetometer plane. This measurement geometry permits connection to the strip line signal leads to the magnetometer chip with a minimum of uncompensated loop area.

The compounds selected for the tests were Lanthinum Hexaboride, and Cerium Hexaboride. Figure 2 shows the waveform and spectral content of Cerium Hexaboride experiment performed in liquid He^3 at 450 mK.

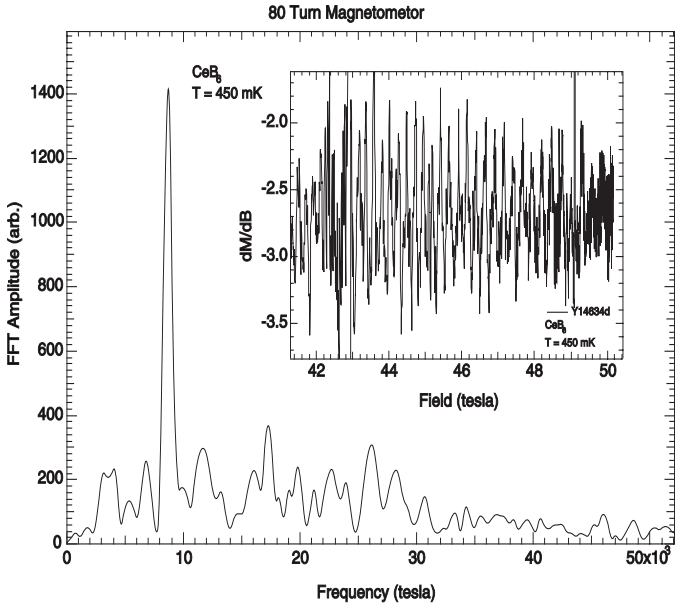

Figure 2. The CeB_6 dHvA signal from the 80 turn magnetometer at 450 mK.

Angular Magnetization and de Haas-van Alphen Measurements to 50 T on $CeRhIn_5$

Cornelius, A.L., LANL
Arko, A.J., LANL
Sarrao, J.L., LANL

We have performed de Haas-van Alphen (dHvA) and magnetization measurements in pulsed fields to 50 T on the tetragonal heavy-fermion antiferromagnet $CeRhIn_5$ as a function of the angle between the crystalline axes of the tetragonal crystal and applied magnetic field. $CeRhIn_5$ is a quasi-2D system that exhibits a field-induced magnetic transition that is first order in nature. We have previously performed dHvA measurements along the <100> and <001> axes and determined that $CeRhIn_5$

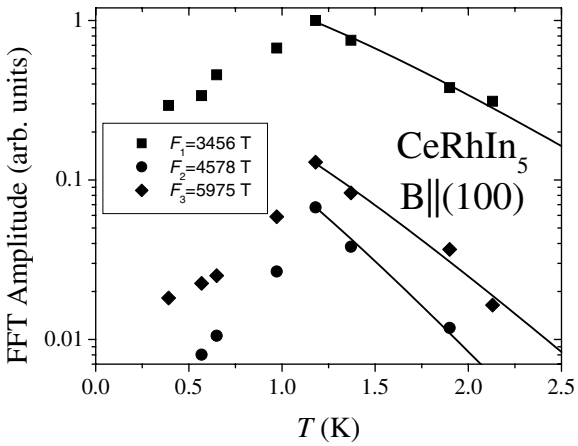

Figure 1. The measured amplitudes of the three dHvA orbits along the <100> axis as a function of temperature.

has an anisotropic Fermi surface. When the field is applied along the <100> axis, three Fermi surface orbits are found. Figure 1 shows the amplitudes of the three dHvA orbits (as determined from fast Fourier transforms of the magnetization versus inverse magnetic field data) along the <100> axis as a function of temperature. As can be seen, the dHvA amplitudes of all three orbits goes through a maximum at T^*=1.2 K. For $T > T^*$, the data can be fit with the standard Lifshitz-Kosevich (LK) theory and effective masses between 5 m_e and 12 m_e were determined. The lines in Figure 1 are fits to the LK theory for the data for $T > T^*$. For $T < T^*$, the amplitudes decrease exponentially which is indicative of a gap in the Fermi surface that requires the carriers to have an activation energy.

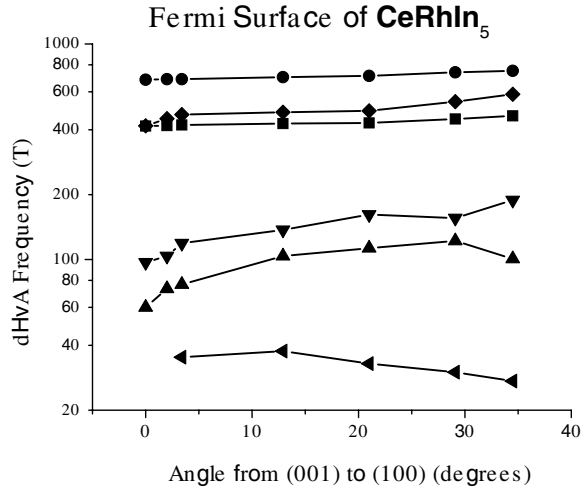

Figure 2. The measured de Haas-van Alphen (dHvA) frequencies as a function of the angle between the cubic crystalline axes and the applied magnetic field in $CeRhIn_5$.

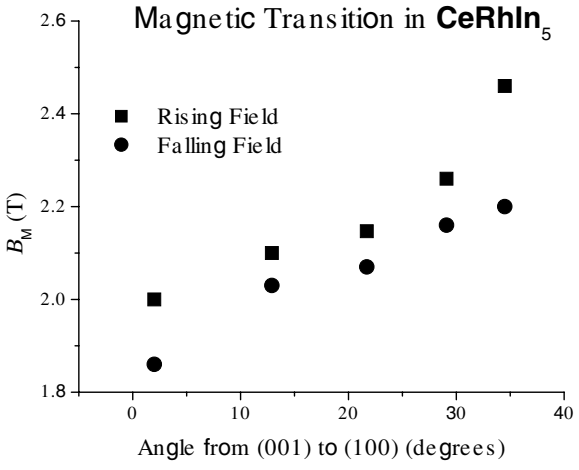

Figure 3. The magnetic field B_M where the field-induced magnetic transition in $CeRhIn_5$ occurs as a function of the angle between the cubic crystalline axes and the applied magnetic field.

We have also started to determine the full 3D Fermi surface of $CeRhIn_5$. Figure 2 shows the results of the dHvA measurements as a function of angle between the crystalline axes and the applied magnetic field. As can be seen, there is not much change in the Fermi surface as a function of angle. Though this is only a partial determination of the Fermi surface, we intend to complete the full set of rotation. To complement the experimentally determined Fermi surface, band structure calculations are also in progress.

$CeRhIn_5$ has 2D antiferromagnet (AF) layers that are weakly coupled to each other. Below T_N=3.8 K, long range AF order is observed. When the magnetic field is applied at the lowest achieved temperature (T~0.4 K) along the easy (001) axis, a magnetic-field induced transition is observed at B_M=2 T. Figure 3 shows the dependence of the magnetic field-induced transition at B_M on the angle between the crystal and the applied field. As can be seen, there is hysteresis between the rising and falling field data indicative of a first order transition. The rise in B_M as the angle is increased from the (001) direction is consistent with the quasi-2D nature of the magnetic structure of $CeRhIn_5$. Since the easy axis is the (001) direction, as the field is applied off the easy axis, a larger applied field will be necessary to induce the magnetic transition.

$Fe_{1-x}Co_xSi$ in High Magnetic Fields

DiTusa, J.F., Louisiana State Univ., Physics
Manyala, N., LSU, Physics
Sidis, Y., LSU, Physics
Aeppli, G., NEC Research Institute
Young, D.P., NHMFL/FSU, Physics
Fisk, Z., NHMFL/FSU, Physics

The Kondo Insulator FeSi attracted attention over 30 years ago because of its unusual magnetic susceptibility (χ).[1] Both χ and the conductivity surprisingly exhibit an activated behavior with the same band gap. Chemical substitution of Co on the Fe site leads to a heavy Fermion metal at ~1% Co concentration[2] where an itinerant helimagnetic (HM) ground state develops.

The magnetic field dependence of the resistivity (ρ_{xx}), the magnetization (M), and the Hall resistivity (ρ_{xy}) in the HM ground state of $Fe_{1-x}Co_xSi$ was measured as shown in Figure 1. We find that M of this compound is similar in form to that of the isostructural and classic itinerant HM MnSi except that it is nearly polarized. ρ_{xy} has a large anomalous contribution presumably due to strong spin-orbit scattering. Furthermore, ρ_{xx}, which is an order of magnitude larger than in MnSi, is insulating like ($d\rho_{xx}/dT < 0$) below the Curie temperature.[3] The magnetoresistance (MR) is strongly positive, opposite in sign from usual itinerant ferromagnets. We have identified the MR as being due to the electron-electron interactions in a disordered HM since our data demonstrate a square-root field dependence at H/T >> 1 (Figure 1c).

[1] Jaccarino, V., *et al*., Phys. Rev., **160**, 476 (1967).
[2] Chernikov, M.A., *et al*., Phys. Rev. B, **56**, 1366 (1997).
[3] Beille, J., et al., Sol. St. Comm., **19**, 399 (1976).

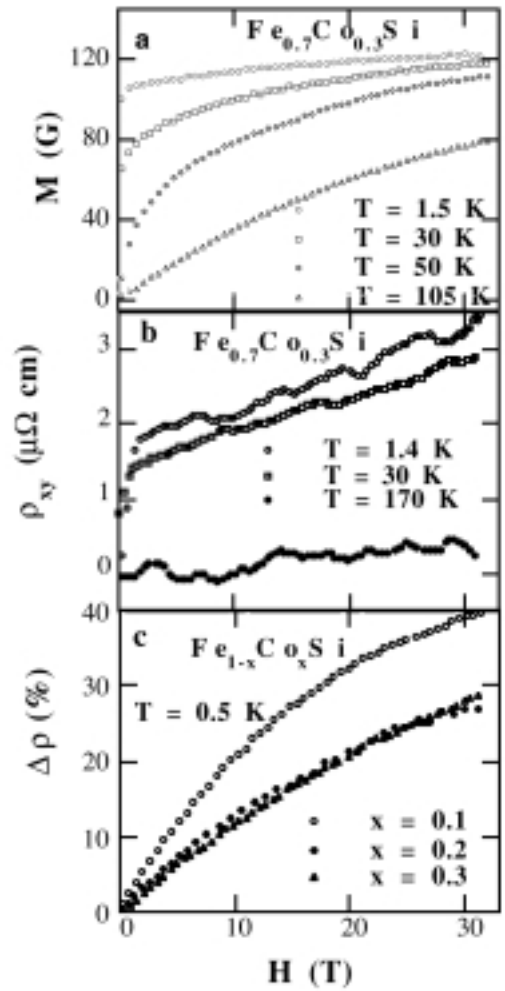

Figure 1. $Fe_{1-x}Co_xSi$ (a) Magnetization x=0.30; (b) Hall resistivity x=0.30; (c) Magnetoresistance x = 0.1, 0.2, 0.3.

Ultrasound Measurements Near the Metamagnetic Transition in UPt_3

Feller, J., Univ. of Wisconsin-Milwaukee and Northwestern Univ., Physics
Ketterson, J.B., Northwestern Univ., Physics
Sarma, B.K., Univ. of Wisconsin-Milwaukee, Physics

High resolution ultrasonic velocity and attenuation measurements have been performed on a single crystal of UPt_3 at the 33 T mK (dil. fridge) facility at NHMFL, Tallahassee. Figure 1 shows the relative velocity (normalized to zero at zero field) of longitudinal sound in the basal plane (b-axis). The magnetic field is parallel to the b-axis. The metamagnetic transition field is ~20.25 T. At low temperatures (below ~1 K) a second velocity dip develops at ~21.7 T. The inset shows the velocity at 70 mK after background subtraction. The frequency of the quantum acoustic oscillations increases rapidly as the transition is approached. The high-field frequency (~9.7 MG) is approximately twice the low-field value and does not correspond to any known de Haas-van Alphen orbit. Analysis

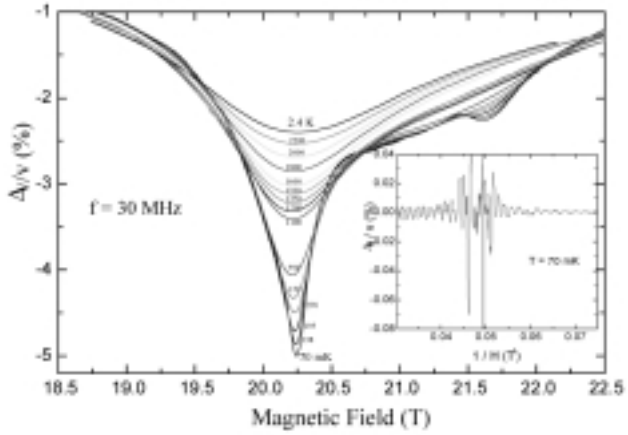

Figure 1. Relative velocity change at the metamagnetic transition showing a new feature at lower temperatures. Inset shows quantum acoustic oscillations.

of the temperature dependence of the oscillation amplitudes at 32 T gives an effective mass ratio of ~31.4.

Acknowledgements: This work was supported by NSF DMR-9704020, 9971123, and 9623682.

Correlated Electron Materials

Fisk, Z., NHMFL/FSU, Physics
Bianchi, A., NHMFL
Drymiotis, F., NHMFL/FSU, Physics
Jackson, D., NHMFL/FSU, Physics
Torelli, M., NHMFL/FSU, Physics

Our research has focussed on further experiments on $YbInCu_4$, the physics of hexaboride materials and the physics of heavy Fermion superconductors. We have as well investigated ferromagnetic properties of the Cr-based planar materials $RCrSb_3$, where R is a rare earth.

(1) Two studies have been carried out on $YbInCu_4$. In a collaboration with Zack Schlesinger (UC Santa Cruz), infrared studies through the 40 K first order, isostructural phase transition have found a feature in the optical conductivity in the mid infrared. Such a feature has been found in several other intermediate valence materials, and the question arises whether this is a signature of intermediate valence, and whether theoretical modeling of the first order transition can produce this feature. A second study in collaboration with the group of Bruno Luthi in Frankfort has measured the elastic properties of $YbIn_{1-x}Ag_xCu_4$ crystals out to Ag concentrations beyond the first order transition boundary. Clear signatures of the phase transition remain in the elastic response well into the region beyond the line of first order transitions. This response can be modeled using the Falicov-Kimball promotional model, and Freericks and Zlatic are applying this theory to the experiments.

(2) A broad range of experiments are continuing in the hexaboride materials, all in collaboration with Ott (ETH Zurich). The weak, high temperature ferromagnetism remains a focus of these efforts. We have found that CaB_6 crystals can be grown with Ca deficiency, leading to hole conductivity and weak ferromagnetism as in the electron doped material. The stoichiometric CaB_6 has been grown with resistance increases on cooling to He temperature from room temperature up to 10^4. The high temperature resistivity of this material has a positive slope above 600 K. The preliminary NMR experiments on the stoichiometric material have found that the relaxation rate is an order of magnitude larger than in the doped, metallic sample. This surprising result appears to support the excitonic insulator picture of the undoped, divalent hexaborides, but no detailed theory is yet available to explain this result. Further deHaas-Van Alphen results on La-doped CaB_6 in collaboration with Hall and Goodrich show a smooth development of the small electron ellipsoids with doping. Further detailed experiments have been done on EuB_6 measurements in magnetic field, as well as Hall effect measurements. The doubling of the plasma frequency below the Curie temperature in EuB_6 appear to be partly due to change in the mass of the carriers, and not primarily a change in carrier density. Optical experiments in collaboration with Degiorgi (ETH Zurich) continue as well on Sm-doped CaB_6 to investigate the evolution of the Kondo insulator state in SmB_6.

(3) Heavy Fermion superconductivity has been the subject of two collaborations. New work on UBe_{13} has been carried out in Ott's group. Andreev reflection measurements give evidence for a p-wave state in this material. Further, specific heat measurements in magnetic field show a scaling behavior that supports this interpretation. A second collaboration with Thompson and Sarrao at Los Alamos has discovered a new class of heavy Fermion superconducting materials based on $CeRhIn_5$ and $CeIrIn_5$. These are compounds not previously reported. They can be grown as large single crystals with high resistance ratios. Superconductivity is induced near 2 K in the Rh compound with 14 kbar pressure, which first suppresses a 3 K Neel state. What is unusual here is that the T_N and T_C are both only weakly pressure dependent, not conforming to the previous cases of pressure induced, heavy Fermion superconductivity where T_c appears after T_N has been pushed toward T = 0 K with pressure. The Ir compound appears to be an ambient pressure heavy Fermion superconductor near 0.4 K. The crystal structure of the compounds consists of layers of $CeIn_3$ and $RhIn_3$. It is possible to prepare related materials with bilayers of $CeIn_3$, and the bilayer Rh material appears to become superconducting under pressure as well. This discovery opens a new materials direction for heavy Fermion superconductivity, one in which the materials allow both Fermi surface and inelastic neutron studies to be made.

Preliminary dHvA Measurements on $La_{1-x}Ce_xRhIn_5$

Goodrich, R.G., Louisiana State Univ., Physics
Hall, D., NHMFL
Sarrao, J., LANL
Fisk, Z., NHMFL

Recently a new layered compound $CeRhIn_5$ has been discovered that is antiferromagnetic at low temperatures and atmospheric pressure and becomes superconducting at high pressures and low temperatures.[1] We performed preliminary measurements of the dHvA effect on 0, 25, and 90 % Ce in $LaRhIn_5$ in an attempt to see changes in the Fermi surface (FS) with doping leading to $CeRhIn_5$. Signals were observed in all three samples, although somewhat reduced in amplitude from pure $LaRhIn_5$.

An example of cantilever torque magnetometry data taken on $LaRhIn_5$ at 1.4 K from 0 to 30 T is shown in Figure 1. In addition to the strong low field oscillations that reach the n = 1 Landau level at approximately 7.5 T, there are a multitude of higher frequencies showing up at higher fields. The 7.5 T oscillations arise from light carriers ($m^* < 0.1$) and are observable up to temperatures on the order of 50 K. The higher frequencies have slightly higher masses and cease to be observable above 10 K. At fields above the n = 1 Landau level the sample takes on a magnetic moment as evidenced by the sharp increase in slope of the output.

We found for the 10 and 25 % La in $CeRhIn_5$ samples that the 7.5 T oscillations did not exist, but there appears to be a progression of the other frequencies between pure $LaRhIn_5$ measured here and pure $CeRhIn_5$ measured previously by Cornelius.[2] Work on this alloy series will continue into the next year.

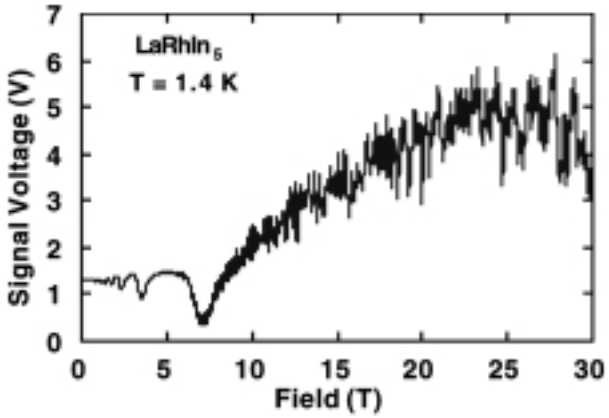

Figure 1. De Haas - van Alphen oscillations in $LaRhIn_5$ taken at 1.4 K using a cantilever magnetometer.

[1] Hegger, H., *et al*., Phys. Rev. Lett., to be published.
[2] Cornelius, A., private communication.

Preliminary dHvA Measurements on $La_{1-x}Sm_x B_6$ and $Ce_{1-x}Ca_xB_6$

Goodrich, R.G., Louisiana State Univ., Physics
Harrison, N., NHMFL
Fisk, Z., NHMFL/FSU

We performed preliminary measurements of the dHvA effect on 5 and 10 % Sm in LaB_6 and 5 and 10 % Ca in CeB_6 in an attempt to see changes in Fermi surface (FS) sizes with doping using lower valency substitutions. Signals were observed in both cases for the 5 % samples, although greatly reduced in amplitude from the pure materials. Very weak signals were observed for $La_{0.9}Sm_{0.1}B_6$ and none were observed for the 10 % Ca in CeB_6 samples.

From the observed frequencies in the 5 % Sm in LaB_6 data we were able to calculate the FS volume and hence the carrier density—interestingly, we found a 5% reduction. In addition, FS ellipsoids appear to no longer overlap because the orbit normally observed from magnetic breakdown ($\alpha_{1,2}$), and much smaller in amplitude than the central smaller orbit (α_3), has an amplitude comparable to the α_3 orbit in these samples. Figure 1 shows a Fourier Transform of the observed signals in the 5% Sm in LaB_6 sample. The lowest frequency peak is the α_3 (ellipsoid minimum area) and the second $\alpha_{1,2}$ (ellipsoid maximum area), and they are nearly of the same amplitude. The next two peaks are harmonics of the first two. This measurement may be the first direct observation of a multi-connected FS changing into isolated pockets with alloying.

We found in two sets of runs for the 10 % Ca in CeB_6 where no data was observed that the sample had been expelled from the pickup coil during a high field pulse. Subsequent magnetic analysis shows that at this concentration, $Ce_{1-x}Ca_xB_6$ has a paramagnetic to ferromagnetic field induced phase transition near 2 T at low temperatures.

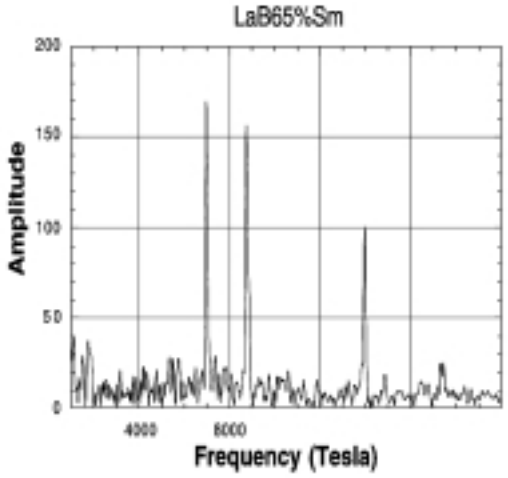

Figure 1. dHvA amplitudes vs. frequencies in $La_{0.95}Sm_{0.05}B_6$.

Magnetoresistance of Single Crystal $U(Pt_{1-x}Pd_x)_3$ with x = 0, 0.002

Graf, M.J., Boston College, Physics
Opeil, C.P., Boston College, Physics
de Visser, A., Van der Waals-Zeeman Institute, The Netherlands
Menovsky, A.A., Van der Waals-Zeeman Institute, The Netherlands
Hannahs, S.T., NHMFL

While the quadratic temperature-dependent resistivity of UPt_3 below 1.5 K is consistent with that expected of a Fermi liquid, the low temperature magneto-resistance (MR) exhibits an essentially linear, not quadratic, field dependence. This linear field dependence has been linked to electron scattering resulting from the onset below 6 K of anomalous "small moment" antiferromagnetism (SMAF).[1] One can test this correlation in single crystals of Pd-substituted UPt_3. Since Pd-substitution enhances the magnetic moment of the SMAF phase, one would expect a corresponding increase in the linear contribution to the MR. We have measured the longitudinal MR for two single crystals with x =0 and 0.002 for current in the a-b plane at T = 100 mK and applied field parallel to the current. The data in Fig. 1 show that the linear term is virtually independent of Pd-concentration, 0.024(1) and 0.026(1) μ cm T^{-1} for x = 0 and 0.002, respectively, even though increasing x from 0 to 0.002 doubles the size of the small ordered moment.[2] Thus the connection between linear MR and the onset SMAF order is questionable. This view is reinforced by our subsequent observation that the longitudinal MR in pure UPt_3 is unchanged within the experimental error by application of 10 kbar pressure, despite the fact that the ordered moment is reduced to zero under pressures of about 6 kbar.[3]

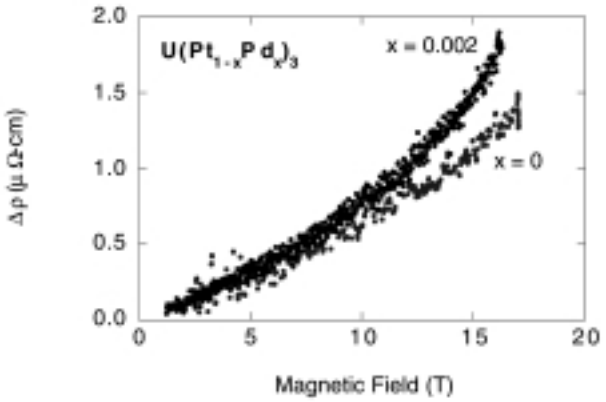

Figure 1. $\rho = \rho(B) - \rho(B=0)$ for two single crystal samples of $U(Pt_{1-x}Pd_x)_3$ at T = 10 mK.

Acknowledgement: This work is supported through Research Corporation award RA0246.

[1] Behnia, K., *et al*., Physica B, **165-166**, 431 (1990).
[2] Keizer, R.J., *et al*., Phys. Rev. B, **60**, 10527 (1999).
[3] Hayden, S.M., *et al*., Phys. Rev. B, **46**, 8675 (1992).

Magnetic Field Dependence of the Paramagnetic to the High Temperature Magnetically Ordered Phase Transition in CeB_6

Hall, D., NHMFL
Fisk, Z., NHMFL
Goodrich, R.G., Louisiana State Univ., Physics

We have measured the magnetic field dependence of the paramagnetic (Phase I) to high temperature magnetically ordered phase (Phase II) transition in CeB_6 from 2 to 30 T using cantilever magnetometry. Cerium hexaboride is one of several rare earth hexaborides that crystallize in the primitive cubic structure with the rare earth ions at the cube center and boron octrahedra at the cube corners. In the past decade there have been many studies of the electronic, thermal, and magnetic properties of CeB_6 because of interest in the low temperature heavy fermion (HF) ground state.[1] All of the magnetic properties arise from the single 4*f* electron on the Ce atom that hybridizes with the conduction electrons to give rise to the HF behavior.

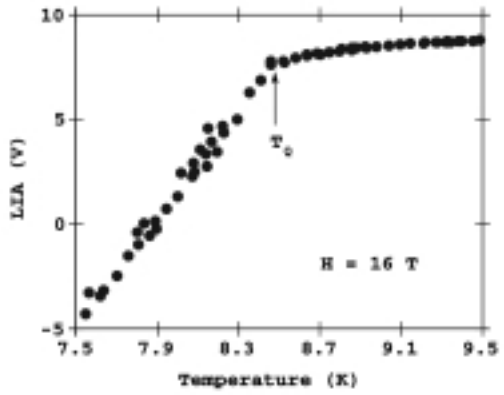

Figure 1. This is an example of raw data taken at an applied magnetic field of 16 T. The temperature was ramped slowly through the Phase I to Phase II transition shown as T_Q on the plot. The change in slope of the capacitance versus temperature curve is taken as T_Q.

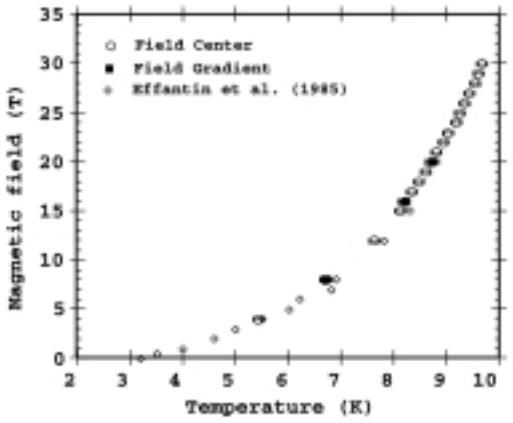

Figure 2. The quadrupolar transition temperature $T_Q(H)$ is shown as a function of magnetic field. New data are compared with previously published data.

Previous measurements of the paramagnetic to high temperature magnetically ordered phase transition were limited to 18 T.[2] All measurements in this study were made with the sample oriented so that the magnetic field was along the <100> axis. The purpose of our measurements was to determine if there is an upper magnetic field limit to Phase II. Several theories predict that large magnetic fields will destroy the magnetic ordering of Phase II.[3] We find that the phase separation temperature continuously increases in field with an increasingly positive slope. In addition, we find that measurements in strong magnetic field gradients have no effect on the phase transition.

The measurements need to be extended to 45 T in order to distinguish between the various theoretical descriptions of Phase II.

1 Schlottmann, P., Physics Reports, **181**, 1 (1989).
2 Effantin, J.M., *et al*., J. Mag. Mag. Mat., **47 & 48**, 145 (1985); Torikachvili, M., *et al.* (unpublished).
3 Uimin, G., Physical Review B, **55**, 8267 (1997); Shiina, R., *et al*., J. Phys. Soc. Jap., **66**, 1741 (1997).

Quantum Oscillations Studies of $U_xTh_{1-x}Be_{13}$ Intermetallics

Harrison, N., NHMFL/LANL
Balicas, L., Venezuelin Institute for Scientific Research; NHMFL/FSU, Physics
Brooks, J.S., NHMFL/FSU, Physics
Teklu, A., Louisiana State Univ., Physics
Goodrich, R.G., LSU, Physics
Cooley, J.S., LANL
Smith, J.L., LANL

Following the successful measurement of the de Haas-van Alphen effect across the entire $Ce_xLa_{1-x}B_6$ series[1], there has been a growing need to explore this possibility in other intermetallic series. One rather interesting series to consider is $U_xTh_{1-x}Be_{13}$, owing to the fact that over certain regions of *x*-space this system exhibits what are thought to be exotic superconducting[2] and non-Fermi liquid ground states[3].

The preliminary work was conducted in pulsed magnetic fields in Los Alamos, leading to a publication concerning the Fermi surface of pure $ThBe_{13}$.[4] It soon became clear, however, that owing to the low frequencies in this material, the most useful data was a achieved at relatively low magnetic fields $B <$ 40 T. Owing to the greater sensitivity of magnetic torque measurements in static magnetic fields, the most successful measurements within this series (at least for $x < 0.1$) were performed in Tallahassee. An example of a magnetic torque measurement of $U_{0.1}Th_{0.9}Be_{13}$ is shown in Figure 1.

Throughout the range $0 < x < 0.1$, the de Haas-van Alphen frequencies were observed to change appreciably, with no notable increase in the effective mass. From the measurements obtained so far we can infer that U enters the $ThBe_{13}$ lattice as

a mixed-valent impurity of mean valence +4.6, implying that the occupation of core-like *5f* states is between that of $5f^1$ and $5f^2$.

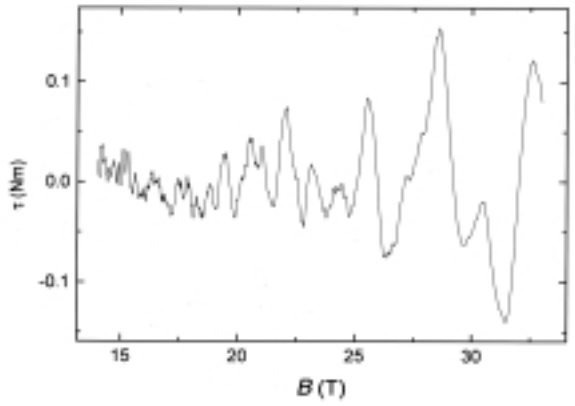

Figure 1. An example of a magnetic torque measurement of $U_{0.1}Th_{0.9}Be_{13}$.

[1] Goodrich, R.G., *et al*., Phys. Rev. Lett., **82**, 3669 (1999).
[2] Ott, H.R., *et al*., Phys. Rev. Lett., **50**, 1595 (1983).
[3] Schiller, A., *et al*., Phys. Rev. Lett., **81**, 3235 (1998).
[4] Harrison, N., *et al*., Phys. Rev. B (in press 1999/2000).

Quantum Critical Behavior in Heavy Fermion Systems

Ingersent, K., UF, Physics/NHMFL
Si, Q., Rice Univ., Physics
Smith, J.L., Rice Univ., Physics

Heavy fermions close to a quantum phase transition have recently been identified as an important class of non-Fermi liquids. Typically, the system is driven from a paramagnetic metal to a magnetic metal by application of external pressure (e.g., $CePd_2Si_2$ and $CeIn_3$) or by chemical substitution (e.g., $CeCu_{6-x}Au_x$). It is widely believed that the magnetic phase transition results from competition between Kondo and RKKY physics. Understanding of this issue, however, is far from complete due to the difficulty of treating on-site and inter-site effects on an equal basis.

We have proposed a quantum phase transition in heavy fermion systems might result from anomalous local Kondo physics. We have put forward an empirical test for such behavior, based on the low-energy behavior of the magnetic susceptibility. Neutron scattering experiments[2] suggest that $CeCu_{6-x}Au_x$ passes this test. We have also demonstrated that a susceptibility of the requisite form can be generated within a model for a single magnetic impurity coupled to a host Fermi system in which incipient magnetic fluctuations give rise to a pseudogap in the quasiparticle density of states. We are now extending the calculations to the lattice using the dynamical mean-field theory of correlated electrons.

[1] Si, Q., *et al*., Int. J. Mod. Phys. B, **13**, 2331 (1999).
[2] Schroder, A., *et al*., Phys. Rev. Lett., **80**, 5623 (1998).

High Field Heat Capacity of $YbInCu_4$

Jaime, M., LANL
Movshovich, R., LANL
Sarrao, J.L., LANL

Metallic $YbInCu_4$ undergoes a first order valence phase transition at 42 K in zero field, where the specific volume is increased by 0.5% upon cooling, with accompanying rise in the Kondo temperature T_K from 25 K to 500 K.[2] It is believed that, unlike in the case of Ce, where the phase transition is described within a Kondo-collapse scenario, the valence transition in $YbInCu_4$ is driven by the band structure effects.[3] The complete magnetic field-temperature phase diagram was obtained in DC Bitter magnets at NHMFL/Tallahassee and in capacitor-driven pulsed magnets at NHMFL/Los Alamos.[4] This work showed that the transition can be suppressed down to T = 0 K with an applied field of 34.3 T.

The magnetic field produced with the long-pulse 60 T magnet is characterized by the low ramp rate of B/ t 400 T/sec, and constant field plateaus of as long as 0.1 sec at 60 T. We have built a probe made mostly of plastic materials, that allows us to perform measurements in vacuum down to a temperature of 1.6 K, in fields up to 60 T. We use a heat pulse method to measure heat capacity, where a known amount of heat is delivered to the sample using a chip resistor as a heater element. The heat capacity of the sample is determined as the ratio of the heat delivered to the sample to the change in its temperature.[1]

In the case of materials that have short thermal relaxation time constants the small thermometer glued to the sample can be in thermal equilibrium with it even during the field ramp. In these cases, if the thermometer reading is plotted vs. magnetic field,

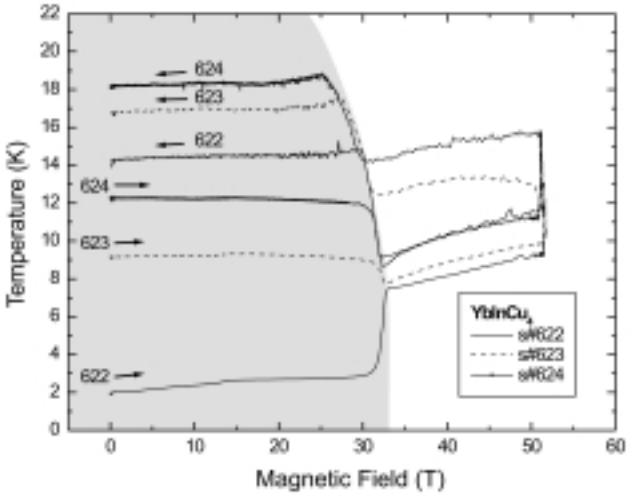

Figure 1. Temperature vs. field plots like this allow mapping off the phase diagram. Here we see little dependence in the magnetic field in the low field phase, a large jump at H = 33 T indicating the phase transition, and a positive slope in the high field phase suggesting a marked magnetic character in this phase. Vertical lines indicate fields at which specific heat data was obtained.

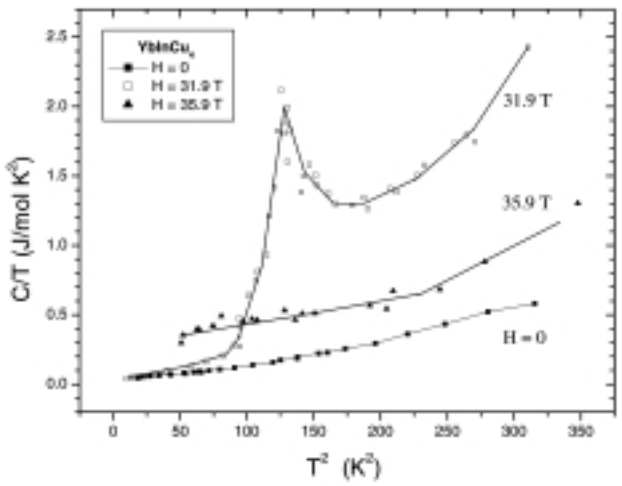

Figure 2. Direct specific heat (C/T vs. T^2) measurements at zero field, 31.9 T and 35.9 T. Measurements in H = 50 T indicated further reduction of the specific heat, to values close C(H=0).

the phase diagram can be mapped, see Figure 1. This mapping is additional information, complementary to the heat capacity data. In this experiment we clearly see the jumps in the sample temperature caused by crossing the phase boundaries. These jumps are a consequence of the nature of the transition, and the adiabatic conditions of the experiment. The irreversibility of the jumps could be related to crystallographic damage (=dissipation) produced to the sample when crossing the phase boundary because of the big change in lattice parameter.[2]

Figure 2 displays the specific heat C/T vs. T^2 measured at constant field in zero field, 31.9 T, and 35.9 T . The data obtained for H = 31.9 T clearly shows the anomaly in the specific heat related to crossing the phase boundary, centered at the temperature predicted from the plot in Figure 1. We also see a substantial increase in the Sommerfeld coefficient as the magnetic field approaches the field required to suppress the phase transition. In addition to all this information our experiment also uncovered unexpected phenomenology. Indeed, shots 622 and 623 in Figure 1 show that the transition changes from exothermic to endothermic between 7 K and 8 K.

1 Jaime, M., *et al*., in *Physical Phenomena at High Magnetic Fields-III*, ed. by Z. Fisk, *et al*., World Scientific, 1999.
2 Cornelius, A., *et al*., Phys. Rev. B, 56, 7993 (1997).
3 Sarrao, J.L., *et al*., Phys. Rev. B, 58, 409 (1998).
4 Immer, C.D., *et al*., Phys. Rev. B, 56, 71 (197).

Specific Heat of $Ce_3Bi_4Pt_3$ Measured in the New 60 T Long Pulse Magnet IHRP

Jaime, M., LANL
Movshovich, R., LANL
Stewart, G.R., UF, Physics
Beyermann, W.P., Univ. of California at Riverside, Physics
Gomez-Berisso, M., Centro Atómico, Bariloche, Argentina
Canfield, P.C., Iowa State Univ., Ames Laboratory
Hundley, M.F., LANL
Sarrao, J.L., LANL

Compounds like CeNiSn, SmB_6, YbB_{12}, and $Ce_3Bi_4Pt_3$ are Kondo Lattice metals at high temperatures. Unlike most *f*-electron compounds, which are metals at low temperatures, in this family a gap in the conduction band opens at the Fermi energy with decreasing temperatures. It has been speculated that the origin of the temperature dependent gap lies in the hybridization between the Abrikosov-Suhl resonance *f* levels and conduction electrons.

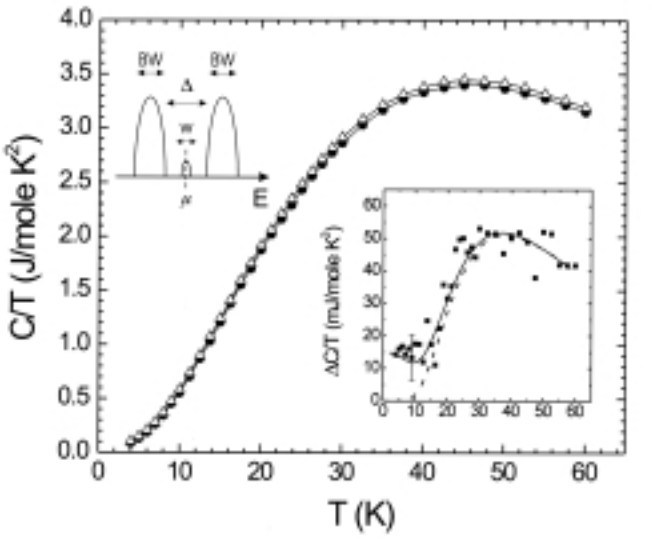

Figure 1. Specific heat C/T vs. T for single crystal sample of $Ce_3Bi_4Pt_3$ measured in zero field (solid circle) and 18 T (open triangle). Inset: Differential heat capacity ΔC/T vs. temperature (solid square) and two fits with the model described in the text (solid and dashed lines).

The band gap in $Ce_3Bi_4Pt_3$ should be observable in the temperature dependence of the specific heat at temperatures comparable to the gap as the conduction band is depopulated. A thermal relaxation technique was chosen to measure the specific heat of a 44.85 mg sample in a superconducting magnet at temperatures between 4 and 60 K. The results of this experiment, C/T vs. T, in zero field and 18 T, are displayed in Figure 1. Subtracting the zero field specific heat C_0 from the specific heat in 18 T (C_{18}) and dividing the difference by the temperature we obtain the differential Sommerfeld coefficient ($\Delta\gamma_{18T}$). $\Delta\gamma_{18T}$, Fig. 1 inset, is rapidly suppressed

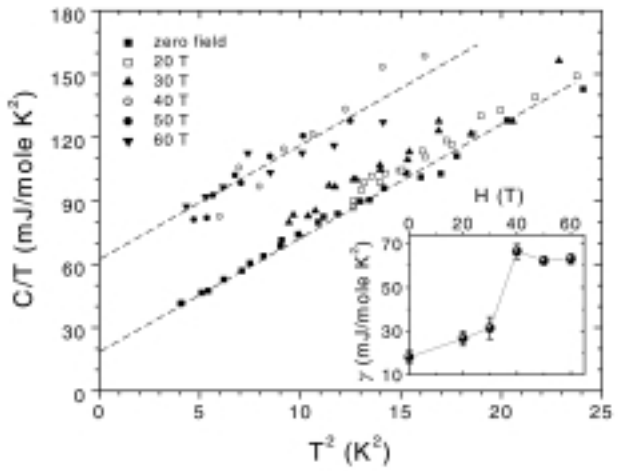

Figure 2. Specific heat C/T vs. T^2 for single crystal sample of $Ce_3Bi_4Pt_3$ in magnetic fields up to 60 T. Inset: Sommerfeld coefficient vs. field.

below 30 K suggesting a change in the magnitude of the gap, and a concomitant loss of charge carriers as the temperature is reduced. We performed a computation for the specific heat of a system with two narrow valence and conductivity bands of equal width BW = 600 K, separated by a gap Δ, and a narrower impurity band of width w = 100 K centered at the chemical potential μ. In this model it was assumed that each band can accommodate 2N electrons, where N is the number of Ce atoms in the sample. The spectral weight of the central band was chosen to reproduce the experimental zero field $\gamma_{H=0}$ when the gap is open, and it is able to accommodate 0.96 % of the total number of states in one band. The difference between calculated specific heat with Δ = 155 K and Δ = 220 K (simulating 18 T and zero field, respectively) is the solid line in the inset of Fig. 1. The quantitative agreement with the data is evident. The difference ΔC remains finite at low temperatures only if some increase of the density of states at the chemical potential is allowed when the gap is reduced. For comparison, a calculation with identical parameters and fixed (field independent) density of states at μ is the dashed line. The finite $\Delta\gamma_{18T}$ indicate that the effect of the applied field is to reduce the gap. The value obtained in our fit for the zero field gap is in excellent agreement with the spin gap Δ_s = 250 K observed in optical experiments.[2]

In addition, we performed direct measurement of the specific heat in $Ce_3Bi_4Pt_3$ at zero field, 20 T, 30 T, 40 T, 50 T and 60 T. The data are displayed in Figure 2. Dashed lines are fits with a fixed phonon term $\beta = 3.6 \pm 0.1$ mJ/mole K[4]. The electronic components are $\gamma_{H=0} = 18 \pm 1$ mJ/mole K[2] and $\gamma_{H=60} = 62 \pm 3$ mJ/mole K[2]. The data obtained at the higher fields indicate little change in γ_H when H > 40 T as shown in Figure 2 inset. The zero field data agree well with earlier experiments. The observed increase in the heat capacity in 40 T is in good agreement with the reversible temperature change during the pulse, caused by adiabatic magnetization. To check the correct operation of the apparatus, specific heat of a Si single crystal was measured in zero field and 60 T. No change in the heat capacity as a function of field was observed, as expected. The Kondo temperature for $Ce_3Bi_4Pt_3$ has been estimated to be T_K 300 K, using the Neutron quasi-elastic line width. An estimate of γ in zero field can be made using the expression of a single impurity spin 1/2 Kondo model[3] $\gamma_0 = 1.29\ \pi R/6T_K$ 50 mJ/moleK[2], value which is in excellent agreement with the observed γ for H 40 T and support a magnetic field induced crossover between Kondo insulator and Kondo metal in $Ce_3Bi_4Pt_3$.

---

1 Jaime M., *et al*., Physica B, in press.
2 Degiorgi L., Rev. Mod. Phys., **71**, 687 (1999).
3 Rajan V.T., Phys. Rev. Lett., **51**, 308 (1983).

UCd_{11} Studied in the New 60 T Long-Pulse Magnet IHRP

Jaime, M., LANL
Movshovich, R., LANL
Sarrao, J.L., LANL

The zero field Sommerfeld coefficient $\gamma = C/T|_{T\_0}$ for UCd_{11} is among the highest in heavy fermion compounds. Additionally, UCd_{11} undergoes a magnetic phase transition around 5 K, whose exact nature is not well understood. Indeed, while μSR experiments are consistent with an antiferromagnetic ordering, the quite symmetric shape of the anomaly observed in the specific heat does not resemble typical antiferromagnetic phase transitions.[1] Moreover, when hydrostatic pressure and magnetic fields are applied to the system, the temperature derivative of the electrical resistivity indicate multiple phase transitions.[2] These transitions could be spin reorientation transitions of the complicated magnetic structure. These results are consistent with the presence of 5*f* electrons in the system that hybridize with the conduction electrons, and are sensitive to magnetic fields and pressure. Recent measurements of the de Haas-van

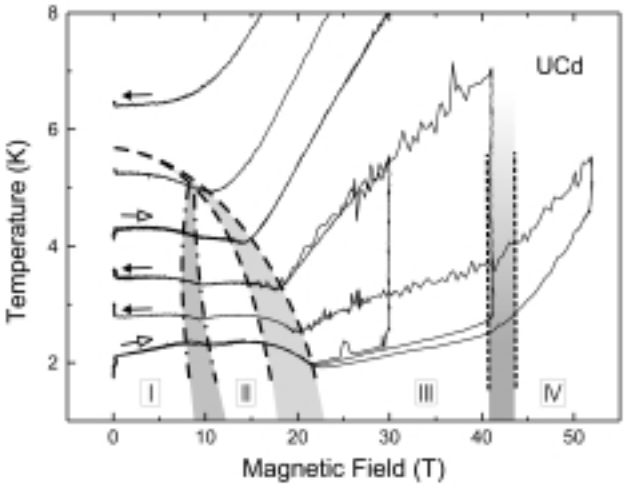

Figure 1. Temperature of a sample of UCd_{11}, in adiabatic conditions, as the magnetic field is pulsed up to 50 T. Grey regions indicate a rapid change of derivative $\partial T/\partial H$ that indicate the opposite change in spin entropy.

Alphen effect in UCd_{11} [3] show evidence for two magnetic field induced transitions at low temperatures, at 6 T and 16 T, compatible with spin reorientation.

We have used our high field calorimeter to measure the specific heat of UCd_{11} up to 50 T. In this report we discuss preliminary data on the evolution of the sample's temperature in adiabatic conditions as a magnetic field of 50 T is cycled. As discussed elsewhere,[4] entropy conservation allows the study of materials in pulsed fields, even in the case where no direct specific heat data is obtained. Figure 1 displays the experimental data. In this plot an increase of the sample temperature as the magnetic field is increased indicates, because of the entropy conservation imposed by the experimental setup, a reduction in the magnetic entropy of the system. Conversely, a decrease of the sample temperature indicates an increase in magnetic entropy. Besides a small initial increase of the temperature in zero field, we see a reduction of the sample temperature in two steps. For the experiment beginning at 4 K the kinks in the T vs. H curves occur at 8 T, and 16 T. These two transitions are compatible with an increase in the spin entropy. This kind of entropy increase is only observed in antiferromagnetically ordered systems that evolve into a canted state. Interestingly, for larger magnetic fields the temperature of the sample increases indicating a reduction in the spin entropy. Such a reduction of the entropy in two steps (regions III and IV in Figure 1) is an indication of new high field magnetic states, reached in a discontinuous fashion as a cascade of magnetic transitions in UCd_{11}. Our experiments confirm previous results and interpretations for the lower fields and uncover a low temperature/high field state not observed until now. Further studies and computation of the specific heat in the different magnetic field regimes are under way.

1 Andraka, B., *et al*., Phys. Rev. B, **44**, 10346 (1991).
2 Thompson, J.D., *et al*., Phys. Rev. B, **39**, 2578 (1989).
3 Cornelius, A.L., Phys. Rev. B, **59**, 13542 (1989).
4 Jaime, M., *et al*. in *Physical Phenomena at High Magnetic Fields-III*, ed. by Z. Fisk, L. Gor'kov and R. Schrieffer. World Scientific, 1999.

Indications of Non-Fermi Liquid Behavior at the Metamagnetic Transition of UPt_3

Kim, J.S., UF, Physics
Hall, D., NHMFL
Heuser, K., Universität Augsburg, Germany, Fachbereich Physik
Stewart, G.R., UF, Physics/NHMFL

The specific heat and resistivity of high purity needle crystals and the magnetization of a 300 mg piece of a Czochralski-process single crystal of UPt_3 aligned so that $B \perp c$ were measured at 0, 18, 19, 20, 22, and 24 T applied fields between 0.5 and 10 K, where $B_{metamag}$ 20 T. The data for C/T, ρ, and χ at 18 T and for C/T and ρ at 24 T indicate that there is still Fermi liquid behavior at low temperatures for B $B_{metamag}$. (For B 21 T, χ displays apparent ferromagnetic behavior). At $B_{metamag}$, however, C/T is found to be proportional to -log T, or characteristic of non-Fermi liquid (nFl) behavior, over more than a decade in temperature while $\rho=\rho_0+AT^{1.2}$ at 22 T (0.5 K T 3 K) and $\chi=\chi_0$-aT at 20.5 T (0.5 K T 20 K)—also both characteristic of nFl behavior. This $C/T \propto$ - log T behavior is a different nFl temperature dependence than previously found for $CeRu_2Si_2$ near its $B_{metamag}$, where C/T was found to decrease linearly with increasing temperature. Thus, although metamagnetism in these, and other, yet to be studied, highly correlated f-electron systems may be a route for attaining long range magnetic interactions that prohibit Fermi-liquid behavior, already the first two systems studied show varying behavior. dHvA data at $B_{metamag}$ for $CeRu_2Si_2$ and SdH data at $B_{metamag}$ for UPt_3, and theories thereof, will be compared. The SdH data shed light on the present χ(H) data for UPt_3 for $B > B_{metamag}$.

Magnetism in Single-Crystalline CePtSn

Nakotte, H., New Mexico State Univ., Physics
Chang, S., NMSU, Physics
Torikachvili, M., San Diego State Univ., Physics
Lacerda, A., NHMFL/LANL
Takabatake, T., Hiroshima Univ., Physics

CePtSn crystallizes in the orthorhombic ε–TiNiSi structure and exhibits two antiferromagnetic transitions at 7.5 and 5 K in zero magnetic field. Using the 20 T superconducting magnet at the Pulse Field Facility, LANL, we determined the phase boundaries of both zero-field phases by means of magnetization and magnetoresistance experiments on single-crystalline CePtSn. The magnetic field was applied along the 3 principal directions. For fields applied along the c-axis, we found that the two magnetic phases are rather insensitive to the application of the magnetic field, in contrast to the behavior for fields applied along the a or b axes, respectively. Anomalies in field scans at fixed temperatures or temperature scans at fixed fields of the magnetization and magneoresistance data were taken to establish the B-T phase diagrams for CePtSn. The results for B//a and B//b are shown in Figure 1a and 1b, respectively. In the figure, diamonds represent the critical values taken from magnetization and circles represent the values determined from magnetoresistance data. Open symbols are taken from field sweeps; solid symbols are taken from temperature sweeps. For comparison, we included previous low-field data (x) from Reference 1. While the phase boundaries of the two antiferromagnetic phases AF1 and AF2 seem to be well established from the present study, there are additional pronounced anomalies in the magnetoresistance with no similar observation in the magnetization (marked with a "?" in the figure). Further studies are needed to identify the origin of these anomalies.

1 Takabatake, T., *et al*., Physica B, **183** 108 (1993).

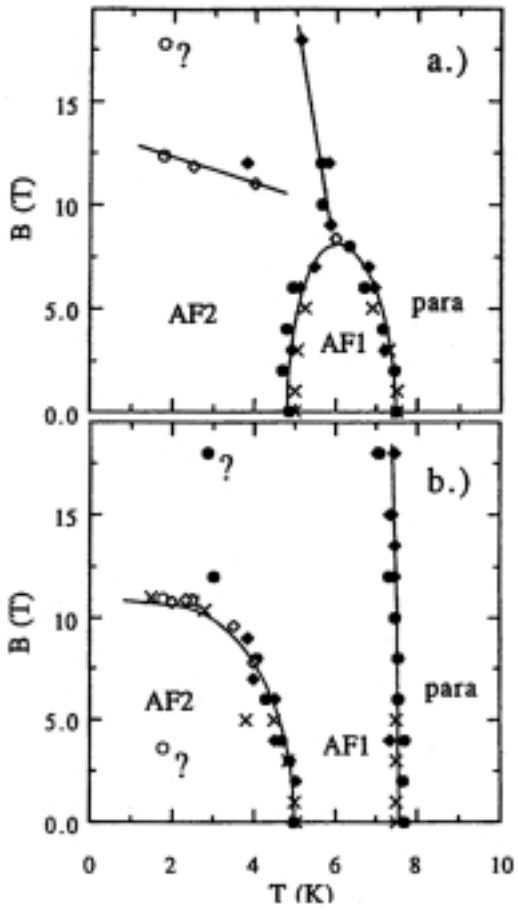

Figure 1. Magnetic phase diagrams of CePtSn for a.) B//a-axis and b.)B//b-axis.

Magnetoresistance and Complex-Conductivity Studies of Small Intermetallic Uranium-Based Single Crystals in Pulsed Magnetic Fields

Nakotte, H., New Mexico State Univ., Physics
Prokes, K., Hahn-Meitner Institute, Berlin, Germany
Chang, S., NMSU, Physics
Bennett, M., NHMFL/LANL
Mielke, C.H., NHMFL/LANL

A common feature of uranium intermetallics is the huge magnetocrystalline anisotropy. For many uranium antiferromagnets, magnetically induced transitions occur in fields that are not accessible with superconducting or continuous resistive magnets. Pulsed magnetic fields are the only alternative. For metallic samples, however, relatively slow dB/dt is required in order to prevent excessive Joule heating and eddy-current shielding. Furthermore, in the case of uranium compounds, single crystals are often very small, i.e. measured quantities are also small. For example, in the case of magnetoresistance measurements, typical voltage changes of the order of a few hundred tenth are needed. This is extremely challenging since the measurements in pulsed magnetic fields are very susceptible to electronic noise during the field pulse.

We tried to optimize the experimental set-up for magnetoresistance measurements on several uranium intermetallics (UNiGe, UIrGe, URu_2Si_2) using the Los Alamos 60-T short-pulse magnet. Unfortunately, we were not able to reduce the background noise to a level that reliable magnetoresistance data could be obtained. We concluded, however, that if the wiring and its shielding were optimized background noise could be reduced by two orders of magnitude to a level at which such measurements would be possible with the present short-pulsed magnets. We believe that the background-noise problems have been fixed when the pulsed magnets moved to the new building in October/November 1999.

Another project was testing the possibility of doing complex-conductivity measurements on such samples. For uranium compounds, the origin of large changes in the transport properties at the field-induced transitions is still heavily discussed (Fermi-surface effects, spin-flip scattering), and complex-conductivity measurements are hoped to provide additional insight. Preliminary results on UNiGe and UIrGe are extremely promising as they show large changes of the complex conductivity at the field-induced transitions in these compounds. This observation is evidence that scattering is not the main origin for the huge magnetoresistance effects.

dHvA Experiments on the Heavy Fermions $CeAl_2$, $CeRu_2Si_2$ and URu_2Si_2

Pricopi, L., Service National des Champs Magnétiques Pulsés (SNCMP) and Laboratoire de Physique de la Matière Condensée (LPMC), Institut National de Sciences Appliquées (INSA) – Centre National de la Recherche Scientifique (CNRS) Toulouse, France
Haanappel, E.G., SNCMP, LPMC, INSA-CNRS
Askanazy, S., SNCMP, LPMC, INSA-CNRS
Lejay, P., Centre de Recherches sur les Très Basses Températures, CNRS, Grenoble, France
Demuer, A., Département de Recherche Fondamentale sur la Matière Condensée (DRFMC), Service de Physique Statistique, de Magnétisme et de Supraconductivité (SPSMS), Centre d'Etudes Nucléaire (CENG), Grenoble, France
Lapertot, G., DRFMC, SPSMS, CENG
Harrison, N., NHMFL/LANL

The quenching of the cyclotron mass of heavy fermion compounds in a strong magnetic field is expected to be a general characteristic of these materials. To verify this we have studied the de Haas-van Alphen effect in three heavy fermion compounds, $CeAl_2$, $CeRu_2Si_2$, and URu_2Si_2, in short-pulsed fields up to 60 T and at temperatures down to 350 mK.

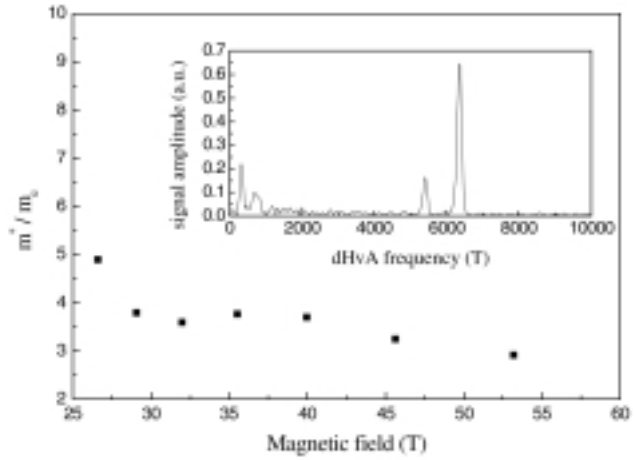

Figure 1. Field dependence of the cyclotron mass of the F = 6.4 kT orbit of $CeAl_2$ with B // [111]. Inset: spectrum of the dHvA oscillations of $CeAl_2$ at T = 590 mK.

The frequency spectrum of $CeAl_2$ with *B* parallel to [111] is shown in the inset of Figure 1. We focus here on the two cyclotron orbits with dHvA frequencies of 5.4 kT and 6.4 kT. Previously we had observed, in fields up to 52 T and at temperatures down to 1.7 K,[1] that their associated cyclotron masses were significantly lower in the field interval between 30 T and 52 T ($m^* = 4.2\ m_e$ for both orbits) than measured by other groups[2] in fields up to 13 T ($m^* = 14.5\ m_e$). The aim of the present experiment was to obtain more precise values of m^* in the interval 30 T to 52 T to demonstrate directly its field dependence, and to bridge the gap between 13 T and 30 T. The measured values of the cyclotron mass for the 6.4 kT orbit are shown in Figure 1. Despite the use of the low temperatures, the lowest field for which we have observed dHvA oscillations was only 25 T. Between this value and the maximum field we have reached, the cyclotron mass decreases gradually with increasing magnetic field.

We have also studied URu_2Si_2, in which no dHvA oscillations could be observed, and $CeRu_2Si_2$. In the latter compound we have observed with *B* // [001] two low-frequency orbits with frequencies of 0.6 kT and 1.1 kT, in good agreement with the previously reported β' and γ' orbits. In our measurements the cyclotron mass of the 1.1 kT orbit was observed to increase with increasing magnetic field. Further experiments are in preparation to examine the origin of this unexpected observation.

[1] Haanappel, E.G., *et al.*, Physica B, **259 – 261**, 1081 (1999).

[2] Springford, M., *et al.*, J. Magn. Magn. Mat., **76 & 77**, 11 (1988); Lonzarich, G., J. Magn. Magn. Mat., **76 & 77**, 1 (1988).

Magnetoresistance of Single-Crystalline UIrGe in High Magnetic Fields

Prokes, K., Hahn-Meitner Institute, Berlin, Germany
Nakotte, H., New Mexico State Univ., Physics
Chang, S., NMSU
Torikachvili, M., San Diego State Univ., Physics
Lacerda, A., NHMFL/LANL

UIrGe crystallizes in the orthorhombic TiNiSi structure and previous single-crystal studies indicate antiferromagnetic ordering below 15.8 K and an additional transition at 14.1 K.[1] For the present work, we have extended the zero-field studies to the application of magnetic fields along the three principal directions using the 20 T superconducting magnet at the Pulse Field Facility, LANL. We performed magnetoresistance studies at various applied fields and temperatures. We found that the magnetic properties of UIrGe are highly anisotropic with the a-axis to be the hard-magnetization axis. However, drastic changes were observed for B//b and B//c. As an example, we show the temperature scans at various fields for B//c in the figure. A clear kink is observed at $T_N = 15.1$ K. Application of a field shifts the ordering temperature toward lower temperatures, and the upturn in resistivity is suppressed for fields larger than ~15 T applied along the c axis. The second zero-field transition at 14.1 K is indistinguishable from present magnetoresistance data below ~10 T (due to the proximity of T_N). At higher fields, however, we observe clear signatures of a second transition. Similar to T_N, also the second ordering temperature is suppressed with increasing field. For B//b, we observe a behavior very similar to B//c except that the critical field is somewhat lower and amounts to ~12.5 T.

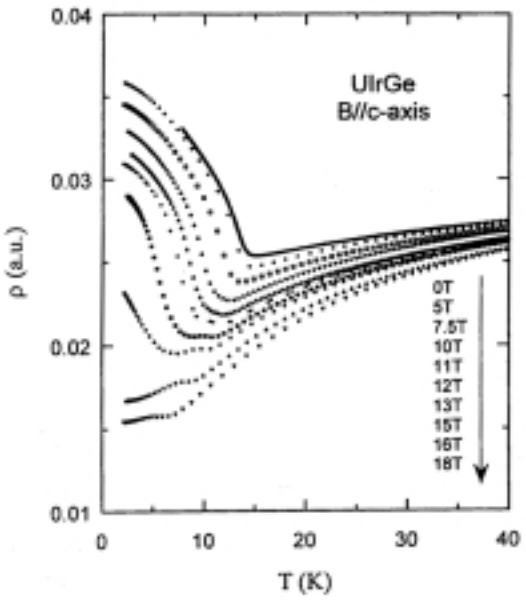

Figure 1. Temperature dependence of the electrical resistivity of UIrGe for i//B//c-axis.

[1] Prokes, K., *et al*., Phys. Rev. B, **60**, 9532 (1999).

Field Suppression of In-Gap Quasiparticle Excitations in SmB_6 IHRP

Reyes, A., NHMFL
Caldwell, T., NHMFL/FSU, Physics
Abdelrazek, M., NHMFL/FSU, Physics
Achey, R., NHMFL/FSU, Physics
Kuhns, P., NHMFL
Moulton, W., NHMFL/FSU, Physics
Fisk, Z., NHMFL/FSU, Physics
Young, D.,* NHMFL

Within the class of strongly-correlated materials, the rare-earth hexaborides exhibit a diversity of phenomena including correlation gap development and dense Kondo behavior. SmB_6, while multivalent at high temperatures and behaving as a narrow d-band metal (Kondo metal), acts as a small gap semiconductor at low temperatures. Mössbauer data on SmB_6 reveals simultaneous presence of (non-magnetic) Sm^{2+} and (magnetic) Sm^{3+} in the ratio of 4:6, which is temperature independent. A hybridized $4f^5 5d^x 6s^y$ state was suggested to explain low temperature susceptibility, where the 6s conduction electron is localized on or near a Sm ion and shields the 4f moment exactly. Low field (1.5 T) NMR measurements[1] on SmB_6 have deduced, from $1/T_1$, a small gap of 50 K in agreement with infrared absorption, inelastic neutron scattering, optical conductivity, and electrical transport. Band structure calculations suggested that small differences in the B-B bond lengths can make SmB_6 behave as a semimetal, as opposed to semiconductor, explaining its low–temperature metallic properties, having a large but finite resistivity below ~4 K. The electronic properties can be attributed to the overlap of a nearly filled boron-based valence band with a nearly empty samarium-based conduction band at one point.

We performed ^{11}B NMR studies of high quality single-crystal SmB_6 for temperatures down to 2 K and in magnetic fields up to 22 T to obtain microscopic information about the ground state.

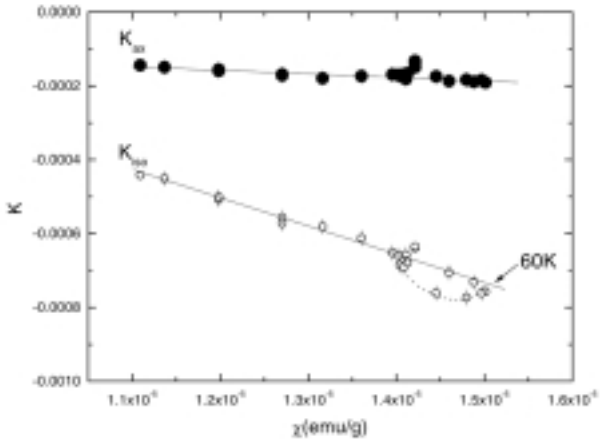

Figure 1. Knight shift vs. bulk susceptibility with temperature as implicit parameter. The relationship is linear at 60 K and above.

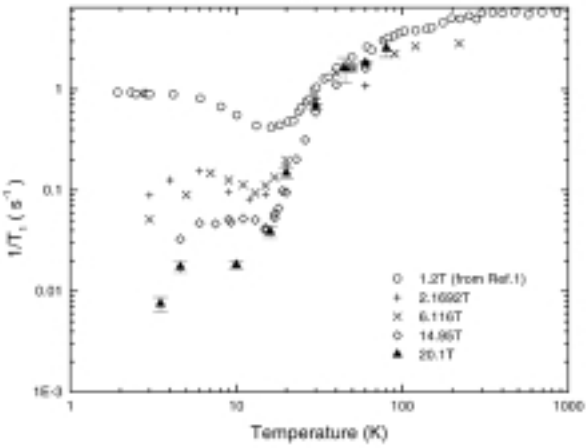

Figure 2. Relaxation rate versus temperature as a function of field.

The Knight shift has a temperature dependence that tracks bulk susceptibility down to 60 K, where susceptibility is greatest. Below this temperature a change in the hyperfine coupling is evident, an anomaly seen in most heavy-electron intermetallics. The isotropic shift reflects the transferred hyperfine field from the Sm ions with hyperfine field of 1.5 kOe/μ_B. The anisotropic part originates from dipolar coupling to Sm moments implying that local moments persist unshielded above the gap temperature. The dipolar hyperfine field Adip = -0.29 kOe/μ_B, in good agreement with the calculated lattice sum value (-0.34 kOe/μ_B), gives a lower bound for Sm saturated moment of 0.16μ_B, well within the predicted 0.28μ_B from Hund's rules. Below 10 K, the relaxation data shows an increase in rate, then saturates. This is believed to be intrinsic since relaxation from local-moment impurities contributes 3 orders of magnitude faster than measured. This T_1 behavior is consistent with the appearance of narrow quasiparticle density of states within the gap just above the Fermi energy as was observed by Raman scattering.[2] The in-gap states are field dependent and are completely suppressed at 20 T. We interpret this to arise from the Kondo-like correlation of localized electronic spins in a low-density carrier system whereby the transport mechanism is governed by hopping from site to site.

* Now at Princeton University

[1] Takigawa, M., *et al*., J. Phys. Soc. Jap., **50**, 2525 (1981).
[2] Nyhus, P., *et al*., Phys Rev. B, **55**, 12488 (1997).

Electrical Resistivity of UBe_{13} in High Magnetic Fields

Schmiedeshoff, G.M., Occidental College, Physics
Palm, E., NHMFL
Hannahs, S.T., NHMFL
Murphy, T., NHMFL
Smith, J.L., Los Alamos National Laboratory

Efforts to experimentally study the heavy fermion ground state of "normal" UBe_{13} are hampered by the appearance of a robust, unusual superconducting state near 1 K.[1] We suppressed the

superconducting state with a large magnetic field and measured the temperature and magnetic field dependence of the electrical resistivity in fields to 32 T and at temperatures to about 45 mK at the NHMFL/Tallahassee.

Our single crystal sample exhibited a superconducting critical temperature of 0.85 K in zero field and an upper critical field of 9.0 T as T→0. These resistive transitions were very sharp: about 7 mK wide in zero field and about 0.4 T wide as T→0, consistent with a very high quality crystal. The field was aligned along the [100] axis.

The transverse magnetoresistance reaches –80% at 1.2 K and 33 T. An inflection point is observed at about 4 T in the 1.2 K data, an inflection point which may be related to a proposed field induced magnetic phase transition in UBe_{13}.[2]

Measurements of the temperature dependence of the resistivity over a temperature range of about 50 mK to 1.1 K were made in several fixed fields from 12 to 32 T. In all fields the resistivity shows the low temperature T^2 behavior characteristic of a Fermi liquid. The temperature at which the resistivity deviates from this quadratic behavior decreases somewhat with increasing field, a behavior which suggests that the zero field ground state of this material is that of a Fermi liquid (unless there is a very strong field dependence to the high temperature limit of the T^2 behavior below 12 T).

It has been noted that the coefficient of the T^2 term in the resistivity (A) is proportional to the square of the coefficient of the T-linear term in the specific heat (γ) in many systems.[3] Thus we expect the effective mass of this material to vary like $A^{1/2}$. Above 25 T we find that $A^{1/2}$ falls off like 1/B, and extrapolates to zero near 54 T. Our results therefore suggest the destruction of the heavy fermion state in UBe_{13} at 54 T. One might expect to see a change in sign of the differential magnetoresistance near 54 T if this suggestion is correct. Measurements in pulse fields are planned to test this prediction.

1 Stewart, G.R., Rev. Mod. Phys., **56**, 755 (1984) and references therein.
2 Schmiedeshoff, G.M., *et al*., Phys. Rev. B, **48**, 16417 (1993).
3 Aronson, M.C., *et al*., Phys. Rev. Lett., **63**, 2311 (1989); and references therein.

Molecular Conductors

Sensitivity of Fermi Surface Traversal Resonance to the Density-Wave Transition in α-(BEDT-TTF)$_2$KHg(SCN)$_4$

Ardavan, A., Univ. of Oxford, Physics
Schrama, J.M., Univ. of Oxford, Physics
Singleton, J., Univ. of Oxford, Physics
Kurmoo, M., Institut de Physique et Chimie des Materiaux de Strasbourg, (IPCMS), France
Day, P., The Royal Institution, London

Among the great variety of groundstates exhibited by metals based on the molecule BEDT-TTF, the groundstate found in α-(BEDT-TTF)$_2$KHg(SCN)$_4$[1] has generated particular interest. This material was generally accepted to form a spin-density-wave at temperatures below about 8 K and magnetic fields below 23 T, but recent work has cast doubt over this;[2] the nature of the density-wave is not clear. It is known, however, that in the low temperature, low magnetic field state, the periodicity of the density-wave causes a reconstruction of the Fermi surface into highly warped quasi-one-dimensional (Q1D) sheets and small quasi-two-dimensional (Q2D) pockets.

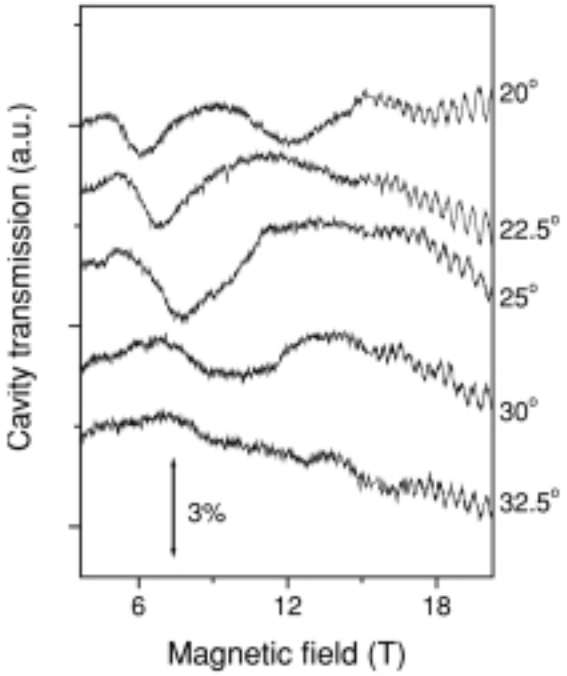

Figure 1. FTR in α-(BEDT-TTF)$_2$KHg(SCN)$_4$; amplitude cavity transmission at 70 GHz and 0.6 K as a function of magnetic field for a range of magnetic field angles from 20 to 32.5 degrees.

We have studied the low temperature, low field state using Fermi-surface traversal resonance (FTR) to characterize the details of the warping of the Q1D sheet.[3] Owing to the Lorentz force, the effect of a magnetic field applied parallel to the plane of the Q1D Fermi sheet is to cause carriers to sweep across the sheet. As they do so, the warping of the sheet causes the real-space velocity of the carriers to oscillate with a frequency that is characteristic of the path taken across the sheet. The oscillatory real-space velocity generates resonances in the high frequency conductivity of the material, $\sigma(\omega)$, when ω matches